LAND SURFACE EMISSIVITIES FOR BRAZIL FROM SSM/I OBSERVATIONS

Rodrigo Augusto Ferreira Souza
Instituto Nacional de Pesquisas Espaciais, Av. dos Astronautas 1758, 12227-010, São José dos Campos, SP.
e-mail: rodrigo@met.inpe.br

Eduardo Jorge de Brito Bastos
Universidade do Vale do Paraíba, Rua Paraíbuna nº 75, Centro, São José dos Campos, SP.
e-mail: ebastos@univap.br.

Regina Célia dos Santos Alvalá
Instituto Nacional de Pesquisas Espaciais, Av. dos Astronautas 1758, 12227-010, São José dos Campos, SP.
e-mail: regina@met.inpe.br

RESUMO

Foram obtidos padrões de rugosidade da superfície do Brasil, para julho e dezembro de 1997, utilizando estimativa de emissividade da superfície em microondas do sensor SSM/I (Special Sensor microwave/Imager) em 19 e 85 GHZ. A contribuição da atmosfera foi estimada usando o modelo ATM (Atmospheric Transmission at Millimetric and sub-millimimetric wavelenghts). As emissividades em microondas foram estimadas a partir da Equação de Transferência Radiativa. As diferenças de emissividade entre os modos de polarização vertical e horizontal foram calculadas para estabelecer o padrão de rugosidade da superfície terrestre. Os resultados mostram que os padrões regionais e sazonais da vegetação são consistentes com a topografia de larga escala e a distribuição da vegetação.

INTRODUCTION

Orbital global observations in the microwave band have been available for the last twenty years, yet there are relatively few studies of the land surfaces that use this kind of data. This is due to the low spatial resolution of the microwave measurements to resolve the spatial patterns of the Earth's surface and to the complex interactions between the regions of cloudiness and the underlying surface. On the other hand, the viewfield of the microwave measurements from satellites is more appropriate to detect scales associated with oceanic and atmospheric variations, what explains the large number of studies over the oceans and the ocean surface itself.

The ocean surface is the largest radiation source measured by an onboard satellite microwave radiometer, and the radiation intensity depends on the surface temperature and emissivity (Lin and Rossow, 1994). The radiances observed by these sensors show differences between the vertical and horizontal polarized brightness temperature. The intensity of the polarized radiation depends on the surface emissivity, with high reflectivity associated with low emissivity. The surfaces that reflect specularly most of the impinging radiation, such as water, have low emissivities while the diffusive reflectors, such as the soil and the vegetation, have large emissivities. As the ocean surface has low emissivity of about 0.5, atmospheric parameters such as cloudiness and liquid water content in the clouds appear with high contrast. There exists good contrast between land and ocean surfaces for the former have emissivities higher than 0.74 (Beer, 1980). Thus, specifying the properties of the ocean surface, the estimates of atmospheric parameters is less susceptible to large errors. However, the estimate of atmospheric parameters over land surface is more difficult due to the high variability of the surface emissivity. This explains the small number of studies with this purpose.

Several studies have emphasize the importance of the Earth's surface emissivity regarding the calibration of sensors onboard the present spatial platforms and the development of new sensors to be launched in the future. In addition other works as those of Wang and Schmugge (1980), Choudhury et al. (1979), Schmugge et al. (1980) and Schmugge et al. (1986) aimed at a better understanding of the responsible mechanisms for the soil and vegetation emission in the microwave band using theoretical analyses and small scale field experiments. Some of these showed that the emissivities of land surfaces are sensitive to the soil and vegetation properties. For larger scale studies one may expect that direct estimates of land surface emissivity yield useful information on the land surfaces, despite the low spatial resolution of the microwave sensors. Therefore, the emissivities may be used to monitor the regional and global scale variations of the properties of the surface and the vegetation.

Most of the studies on the microwave emission from the soil and vegetation focus on the use of simple indices, such as the MVI (Microwave Vegetation Index) which is based on the polarization difference for the 37 GHz channel: for each month, the temporal differences of polarization are ordered and the second smallest value is retained so to maximize the response of the vegetation and minimize the moisture and cloudiness effects (Prigent,

1997). The MVI index has been largely employed to monitor the vegetation and floods using observations from the multi-channel radiometer in the microwave band, SMMR (Scanning Multi-channel Microwave Radiometer) and from the SSM/I sensor as described in Choudhury et al. (1987), Choudhury and Tucker (1987), Choudhury (1988, 1989), Justice et al. (1989), Tucker (1992) among others.

More recently Prigent et al. (1997) estimated the land surface microwave emissivity for March, July, October and December, 1991 for Africa, most of Europe and western Asia. They used the solution of RTE and SSM/I data onboard the F10/DMSP satellite. In addition, ISCCP (International Satellite Cloud Climatology Project) surface temperature data and moisture and temperature profiles inferred from the TOVS/TIROS-N (TIROS Operational Vertical Sounder) were used in order to remove the atmospheric contributions (absorption and scattering) including that from the clouds. Their results showed that the vegetation, topography, snow coverage and soil moisture do affect the estimates of land surface emissivity.

Generally, the land surface emissivity changes with the texture, composition and water content of the soil. However, the spectral region of detection, the geometry of the sight and the surface absolute temperature are factors that also change the emissivity. The determination of the emissivity in the microwave band is important not only for a continuous monitoring of land surfaces using remote sensing techniques but also because it is an relevant physical parameter of the medium.

The objective of this study is to estimate land surface emissivity for the entire Brazilian territory using satellite microwave data for July and December, 1997. The importance of this study resides in the importance of these estimates and its subsequent utilization in radiative transfer models in the microwave band for applications in remote sensing of the surface and the atmosphere. One solution of the RTE, data SSM/I onboard the F14/DMSP satellite and TOVS data onboard TIROS-N/NOAA satellite series will be used. This study also includes the evaluation of the roughness pattern of the Brazilian territory basing on the difference between the fields of vertically and horizontally polarized emissivity, using the land surface emissivity data obtained in the previous stage.

DATA

Brightness temperature data obtained from the SSM/I sensor onboard the F14/DMSP satellite (Hollinger et al., 1987 and Hollinger et al., 1990) and surface skin temperature data from the system TOVS/TIROS-N (TIROS Operational Vertical Sounder) were used in this study. The TOVS data, collected at the Divisão de Satélite Ambiental – DAS (Division of Environmental Satellite) of the Instituto Nacional de Pesquisas Espaciais (National Institute for Space Research) in Cachoeira Paulista, SP, Brazil, cover the region within (5°S,40°S) and (30°W, 80°W). The data refer to the months of July and December and the study area is the entire Brazilian territory.

METHOD

The solution of the RTE for a parallel plane atmosphere with no scattering over a plane surface can be expressed in terms of the brightness temperature for each orthogonal polarization P (P indicates either the horizontal polarization, PH or the vertical polarization, PV). Starting from RTE has the following equations:

$$TbP = T_S\ \varepsilon_P\ e^{-\tau(0,s_1)\sec\theta}\ + T_{atm}{}^{\downarrow}\ (1-\varepsilon_P)\ e^{-\tau(0,s_1)\sec\theta}\ + T_{atm}{}^{\uparrow} \tag{1}$$

and

$$TbP_V - TbP_H = \left(T_S - T_{atm}{}^{\downarrow}\right) e^{-\tau(0,s_1)\sec\theta}\ \left(\varepsilon_{P_V} - \varepsilon_{P_H}\right), \tag{2}$$

where

$$T_{atm}{}^{\downarrow} = \int_0^{s_1} T(z)\ r\ k(z)\ e^{-t(0,z)\sec q}\ \sec q\ dz \tag{3}$$

and

$$T_{atm}{}^{\uparrow} = \int_0^{s_1} T(z)\ r\ k(z)\ e^{-t(z,s_1)\sec q}\ \sec q\ dz, \tag{4}$$

where TbP is the brightness temperature for the polarization P; Ts, the surface skin temperature; εP, the surface emissivity for polarization P; θ, the view angle of the satellite; ρ, the atmospheric density; k(z), the atmospheric absorption coefficient for a given altitude z; T(z), the atmospheric temperature at altitude z; and $\tau(z_0, z_1) = \int_{z_0}^{z_1} \rho\, k(z)\, dz$, the atmospheric opacity between z0 and z1.

Isolating the terms in the Equations 1 and 2 that correspond to the surface emissivity, one obtains the following equations:

$$\varepsilon_P = \frac{TbP - T_{atm}^{\uparrow} - T_{atm}^{\downarrow} e^{-\tau(0,s_1)\sec\theta}}{e^{-\tau(0,s_1)\sec\theta}\left(T_S - T_{atm}^{\downarrow}\right)} \qquad (5)$$

and

$$\varepsilon_{P_V} - \varepsilon_{P_H} = \frac{TbP_V - TbP_H}{e^{-\tau(0,s_1)\sec\theta}\left(T_S - T_{atm}^{\downarrow}\right)}. \qquad (6)$$

Equations 5 and 6 were used in the present study to determine the surface emissivity in polarizations P and the surface roughness patterns, respectively.

APPLICATION OF THE METHOD

Initially the SSM/I images for the region (10°N, 40°S) and (30°W, 75°W), that is, over Brazil were selected. Four passages of the F14/DMSP satellite were selected for each day, what totals 248 passages for July and December. Once the images were selected, the satellite projection was transformed into grid points, with the generation of files containing latitude, longitude and brightness temperature, in the spatial resolutions corresponding to the frequencies of 19 and 85 GHz.

Subsequently, TOVS soundings were selected according to the passage times of the F14/DMSP over Brazil, so to have NOAA-12 and NOAA-14 soundings coincident with those of the F14/DMSP. The processing of the TOVS soundings were made using the ITPP5.0 software, resulting in surface temperature files for cloud free areas. Next, the surface temperature data were transferred to the grid points in the resolutions of 0.25° x 0.25° and 0.5° x 0.5°. However, due to a difference in the passage times of the NOAA-12, 14 and F14/DMSP satellites it was necessary to consider the monthly averaged surface temperature fields for the morning, late afternoon and nighttime hours. Errors of the order of 5K in the estimates of the surface temperatures imply changes less than 2 % in the estimates of the emissivity. Therefore, the use of monthly averaged surface temperature fields for the determination of the emissivity is quite valid.

The ITPP5.0 is a computational package used to infer vertical temperature and moisture profiles from the processed information obtained by the HIRS-2 and MSU sensors of the TOVS system (Werbowetzki, 1981). This package was developed by CIMSS (Cooperative Institute for Meteorological Satellite Studies) of the University of Wisconsin, Madison. These information are transmitted by the NOAA satellite, multiplexed with the data from the AVHRR sensors, and other kinds of data pertinent to the mission of the satellite (surface skin temperature, for example). Data from channel 8 of the HIRS-2 (atmospheric window) were used. It must be pointed out that the ITPP5.0 assumes that the surface temperature is equal to the brightness temperature for clear sky conditions.

The monthly averaged surface temperature fields were obtained using the Krining interpolation method. In addition, a mask was used to interpolate the surface temperature values only to the grid points within the Brazilian territory, thus minimizing possible interpolation errors in the continent/ocean. boundary.

The parameters Tatm↑, Tatm↓ and τ were obtained from simulations with the ATM (Atmospheric Transmission at Millimetric and sub-millimetric wavelengths) model. The satellite observation mode in 19 and 85 GHZ was utilized, assuming a tropical standard atmosphere for the entire Brazilian territory. The ATM, modified later by Pardo (1996), permits to calculate the atmospheric opacity (optical thickness), for each frequency and for different layers, using the atmospheric temperature and pressure and the types of molecules (H_2O, O_2, trace gases).

The calculation of the emissivity was performed using Equation 5, which were estimated in the horizontal and vertical polarizations for each passage of the F14/DMSP satellite. The emissivity files were grouped together to produce the monthly mean field for the Brazilian territory. Values less than 0.74 were filtered out from each emissivity file and the grid points with the presence of clouds or water were not considered in this field. Furthermore, for the grid points with more than one value of emissivity an arithmetic average was performed. The threshold of 0.74 was chosen with basis on the results of Beer (1980) and Prigent et al. (1997).

Finally, the subtraction of the emissivity field in the horizontal polarization from that in the vertical polarization was done to determine the roughness pattern of the surface, accordingly to Equation 6.

RESULTS

The emissivity fields in 85 GHz, in vertical and horizontal polarization modes are shown in Figures 1(a) and 1(b), respectively. For both polarizations, the largest emissivity values are found over the North and Northeastern regions. The lowest values are found in different sub-regions of the country, such as the Amazon Basin, Pantanal and in small areas in the South and Southeastern regions. The low emissivity values may be associated with the cover and/or characteristics of the terrain, as for example non-vegetated or barely vegetated areas. These results are similar to those found by Prigent et al. (1997) for some regions of the African continent. It can be noted that the emissivity values in the vertical polarization are slightly larger than those in the horizontal polarization. This means that the horizontal polarization is more appropriated to identify areas with low land surface emissivity.

In Figs. 2(a) and 2(b), respectively, the 19 GHz emissivity fields for both horizontal and vertical polarization modes show a relatively smoother pattern when compared to those of 85 GHz. The North (in particular the Amazon Basin) and the Central western (in particular, the Pantanal) regions show the smallest emissivity values for the entire Brazilian territory, which are associated with the characteristics of the terrain, because these regions may be considered flat surfaces when compared to vegetated areas, at the sensor's spatial resolution. It can be also noticed that the emissivity values in the vertical polarization are higher than those in horizontal polarization, a characteristic also observed in the 85 GHz emissivity fields.

In Figs. 3(a) and 3(b), respectively, the December 85 GHz emissivity fields both in horizontal and vertical polarization modes show a different pattern from that of July. The largest differences are over the South region and the states of São Paulo and Mato Grosso do Sul. On the other hand, a decrease (0.02) in the emissivity values over the North region, mainly over the Amazon Basin could be noted. In Figs. 4(a) and 4(b) the 19 GHz emissivity fields in both polarization modes show a similar pattern to that of July, with higher emissivity values in both modes, respectively.

The comparison of the land surface emissivity for July and December reveals a seasonal variation, with higher values during December. This variation in the emissivity field may be associated with land cover changes (biomass density). The emissivities in both polarization modes decrease with increasing frequency. This trend is more conspicuous over barely vegetated areas such as those of the South and Central western Brazil. These same characteristics were also observed by Prigent et al. (1997) for some regions of the African continent.

The estimation of the land surface emissivity for some ocean areas was made in antecipation to the determination of this parameter over land surfaces. The values found varied between 0.30 and 0.69 approximately. These values are consistent with those of Beer (1980), who estimated values between 0.33 and 0.60 for calm waters.

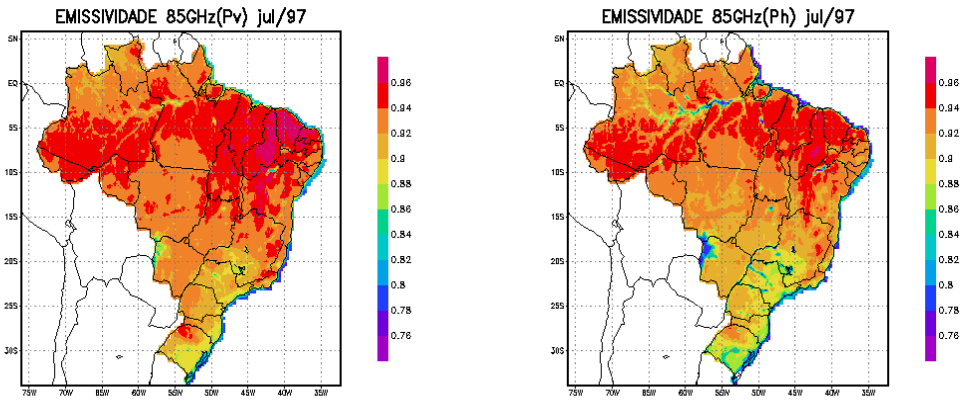

(a) (b)

Figure 1 - Emissivity at 85 GHz for July: a) vertical polarization, b) horizontal polarization.

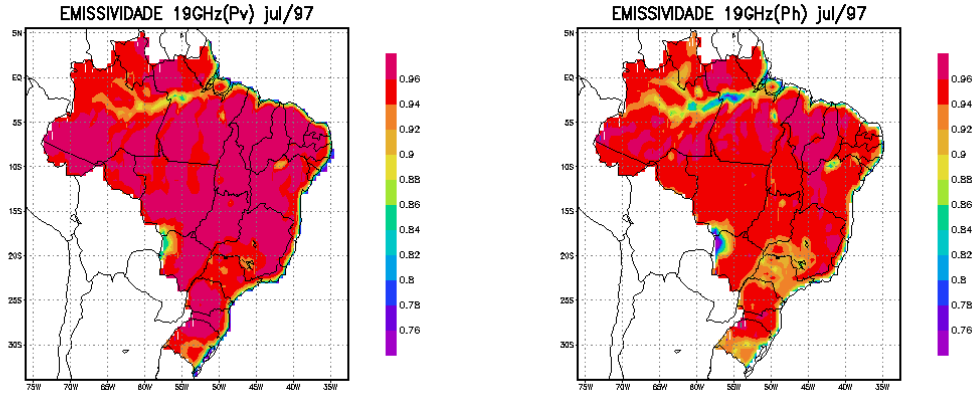

(a) (b)

Figure 2 – Emissivity at 19 GHz for July: a) vertical polarization, b) horizontal polarization.

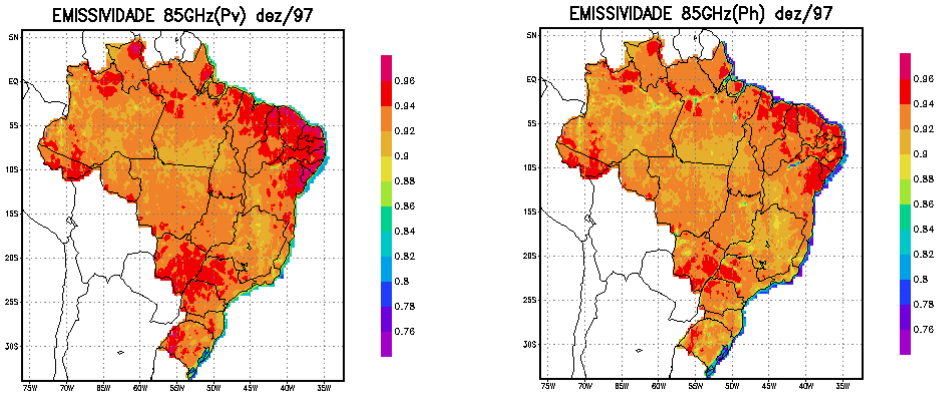

(a) (b)

Figure 3 – Emissivity at 85 GHz for December: a) vertical polarization, b) horizontal polarization.

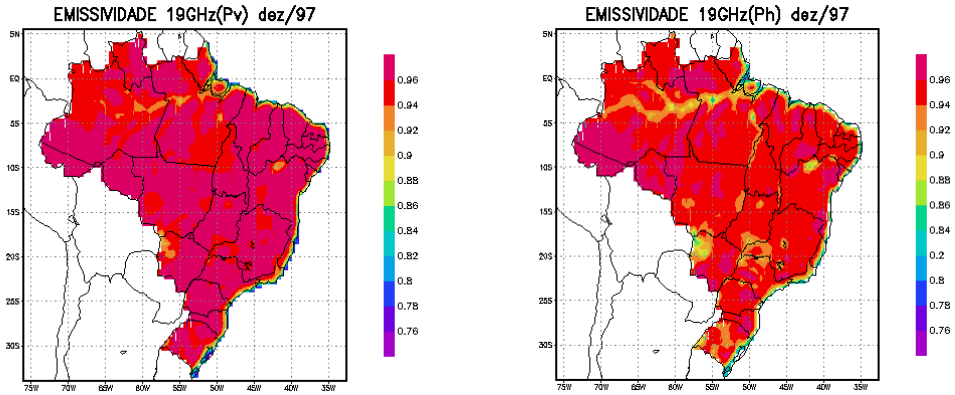

(a) (b)

Figure 4 – Emissivity at 19 GHz for July: a) vertical polarization, b) horizontal polarization.

In Fig. 5(a) the 85 GHz difference field corresponding to July shows the smallest values over the North region (Amazon Florest) although there exists a narrow stripe of maximum values stretching from the western side of the Basin toward the Atlantic Ocean. Other maxima are also observed over the Pantanal (Central western region), north of Bahia state and the southwestern part of the Southeastern region. The largest values of the emissivity differences are associated with the characteristics of flat surfaces (water, non-vegetated or barely vegetated areas) while the lowest values are related to rough surfaces (vegetated and/or mountainous areas). These characteristics were also observed by Prigent et al. (1997) for the African continent. The roughness pattern for

19 GHz (Fig. 6a) is similar to that of 85 GHz but smoother due to the lower spatial resolution of the grid (0.5^o x 0.5^o). Similar patterns are also observed for December in both frequences in Figs. 5(b) and 6(b).

Generally, there is a difference between the roughness patterns of July and December. A considerable increase in roughness is observed in December, although for the North region it is not as significant as in the rest of the country. This increase depends on the type of vegetation and may be characterizered by the vegetation classification. With the decrease in the biomass density, the horizontal polarization decreases and the vertical polarization increases, thus increasing the difference between the polarization modes. This characteristics was also observed by Prigent et al. (1997).

The same seasonal variation of the vegetation is noted when the emissivity difference fields of December and July are compared with the Leaf Area Index (LAI) presented by Ranga et al. (1997). Therefore it seems plausible that the increase in roughness [Figs. 5(b) and 6(b)] is directly related to the increase in biomass density.

Another observed characteristics was the presence of low emissivity difference values near the eastern coast of Brazil, both in July and December, which may be associated with the topographic characteristics of the region (mountainous). When the emissivity difference fields of July and December are compared to the digital topographyc map of South America, elaborated by EROS (Earth Resources Observation Systems) Data Center, one notices that low difference values are found over the mountainous regions near the eastern of Minas Gerais and Bahia states.

The emitted energy by rough surfaces is strongly scattered in all directions. In extreme cases of very rough surfaces the energy is equally scattered (Elachi, 1987), thus causing the emissivity difference to decrease as the topography becomes rougher. These characteristics are difficult to be estimated for vegetated areas because the vegetation usually changes the topography and the emissivity difference becomes low (Lambertian behaviour). In the spatial scales used in this study, the rocky or barely vegetated surfaces act as a flat, homogenous surface causing the emissivity differences to be high.

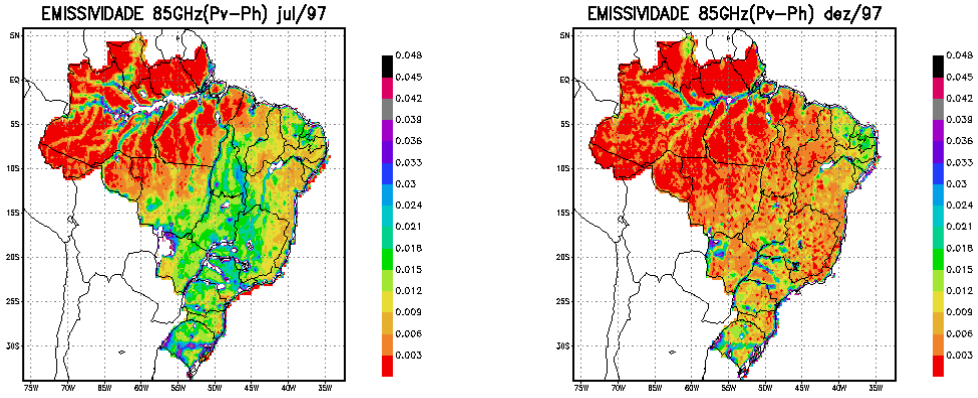

(a) (b)

Figure 5 – Surface roughness pattern at 85 GHz: a) July and b) December.

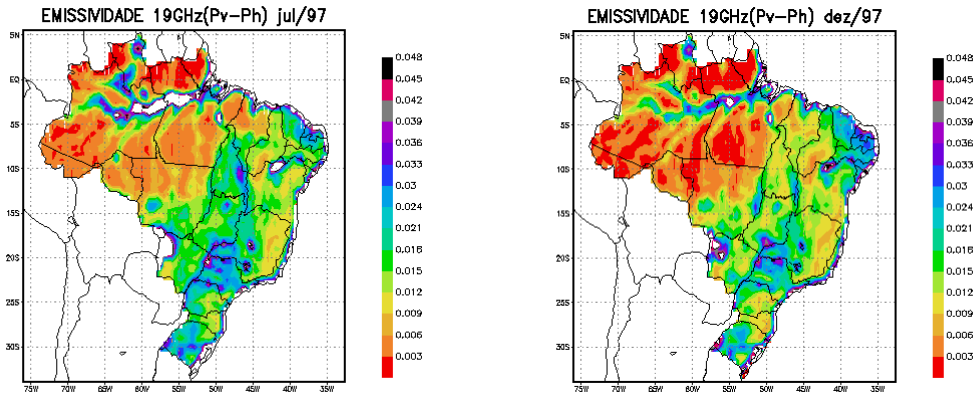

(a) (b)

Figure 6 – Surface roughness pattern at 19 GHz: a) July and b) December.

CONCLUSIONS

In the absence of direct measurements of surface emissivities at these larger spatial scales, these results show that the regional patterns and seasonal changes of the retrieved emissivities are compatible with large-scale topography and vegetation distribuitions, and with flooding events, lakes and rivers. The emissivity sazonal variation can been associated with modifications in the vegetation cover (biomass density).

The regions of bare soil and rock show low emissivities at horizontal polarization ($0.80 < \varepsilon < 0.88$) and high polarization diffrences ($\varepsilon_v - \varepsilon_h > 0.015$), compared to vegetated areas. At the spatial scales (0.25° x 0.25° and 0.5° x 0.5°), bare soil act as a smooth surface, producing high polarization differences associated with quasi-specular reflection. On the other hand, densely vegetated zones (the tropical Amazon forest for instance) exhibit high emissivities at horizontal polarization and low polarization differences because of scattering by the vegetation. For sparsely vegetated or unvegetated areas the polarization differences decrease with increasing topographic roughness. In coastal areas where a substantial portion of the SSM/I pixel may include ocean, low emissivities are associated with high polarization differences (ocean in the “side lobes” of the SSM/I antenna pattern can also cause na underestimate of the microwave emission for coastal pixels).

Different roughness scales may be involved within a single field of view, from the small-scale roughness related to surface irregularities, small compared to the wavelength, to the large-scale topographic effects. The effect of topography is to locally modify the viewing angle with respect to the horizontal and vertical polarizations as defined for a flat surface. Within a field of view, different surface slopes related to topography tend to mix the vertical and horizontal polarizations as defined relative to the mean flat surface. Thus with increasing topography roughness, the reflection properties of the surface approaches a lambertian behavior. In vegetated areas this feature is difficult to evaluate, first because the vegetation usually changes with the topography, and second because the emissivity difference in polarizations is already low.

In the microwave, flooding produces a decrease in emissivities in both polarizations but an increase in the polarization differences, especially at lower frequencies, because of the differences in dielectric properties of water and soil or vegetation. Modeling of the various land surfaces and comparisons with retrieved emissivities further understand the complex physics of surface emissivities, possibly to invert the radiative transfer equation to retrieve soil, vegetation and atmospherics parameters.

REFFERENCES

LIN B. and ROSSOW W. B. Observations of cloud liquid water path over oceans: optical and microwave remote sensing methods. **Journal of Geophysical Research**, v. 99, pp. 20907-20927, 1994.

BEER T. Microwave Sensing from Satellites. **Remote Sensing of Environment**, v. 9, pp. 65-85, 1980.

WANG J. R., SCHMUGGE T. J. An empirical model for the complex dielectric permittivity of soils as a function of water content. **IEEE Transactions on Geoscience and Remote Sensing**, GE-18, pp. 288-295, 1980.

CHOUDHURY B. J., SCHMUGGE T. J., NEWTON R. W. and CHANG A. Effect of surface roughness on the microwave emission from soils. **Journal of Geophysical Research**, v. 84, pp. 5699-5706, 1979.

SCHMUGGE T. J., JACKSON T. J. and MCKIM H. L. Survey of methods for soil moisture determination. **Water Resources Research**, v. 16, pp. 961-979, 1980.

SCHMUGGE T. J., O’NEILL P. E. and WANG J. R. Passive microwave soil moisture research. **IEEE Transactions on Geoscience and Remote Sensing**, v. 24, pp. 12-22, 1986.

PRIGENT C., ROSSOW W. B. and MATTHEWS E. Microwave land surface emissivities estimated from SSM/I observations. **Journal of Geophysical Research**, v. 102, N°.D18, pp. 21867-21890, 1997.

CHOUDHURY B. J., TUCKER C. J., GOLUS R. E. and NEWCOMB W. W. Monitoring vegetation using Nimbus-7 scanning multichannel microwave radiometer's data. **International Journal of Remote Sensing**, v. 8, pp. 533-543, 1987.

CHOUDHURY B. J., TUCKER C. J. Monitoring global vegetation using Nimbus-7 37 GHz data. Some empirical relations. **International Journal of Remote Sensing**, v. 8, pp. 1085-1090, 1987.

CHOUDHURY B. J. Microwave vegetation index: a new longterm global data set for biospheric studies. **International Journal of Remote Sensing**, v. 9, pp. 185-186, 1988.

CHOUDHURY B. J. Monitoring global land surface using Nimbus-7 37 GHz data. Theory and examples. **International Journal of Remote Sensing**, v. 10, pp. 1579-1605, 1989.

JUSTICE C. O., TOWNSHEND J. R. and CHOUDHURY B. J. Comparison of AVHRR and SMMR data for monitoring vegetation phenology on a continental scale. **International Journal of Remote Sensing**, v. 10, pp. 1607-1632, 1989.

TUCKER C. J. Relating SMMR 37 GHz polarization difference to precipitation and atmospheric carbon dioxide concentration: A reappraisal. **International Journal of Remote Sensing**, v. 13, pp. 177-191, 1992.

HOLLINGER J. P., LO R., POE G. A., SAVAGE R. and PIERCE J. L. **Special Sensor Microwave/Imager user`s guide**. Nav. Res. Lab. Washington, D. C., 1987.

HOLLINGER J. P., PIERCE J. L. and POE G. A. SSM/I instrument evaluation. **IEEE Transactions on Geoscience and Remote Sensing,** 28, pp. 781-790, 1990.

WERBOWETZKI A. **Atmospheric sounding user's guide**. Washington, DC, NOAA, Apr. 1981. (NOAA Techical Report NESS 83).

PARDO J. R. **Études de l'atmosphère terrestre au moyen d'observations dans les longues d'onde millimétriques et submillimétriques** p.Tese de Doutorado - Universidad Complutensede Madrid, 1996.

RANGA B. M., NEMANI R. R. and RUNNING S. W. Estimation of Global Leaf Area Index and Absorbed Par Using Radiative Transfer Models. **IEEE Transactions on Geoscience and Remote Sensing**, v. 35 (n. 6), pp. 1380-1393, 1997.

ELACHI C. **Introduction to the physics and techniques of remote sensing**. NewYork, John Wiley and Sons. Inc., 1987.